

Template Waveform Synthesize Technique for Ultra-wide band Signal in Measuring Distance

1st Nguyen Thi Huyen
Le Quy Don Technical University
 Ha Noi, Viet Nam
 nguyenhuyen@mta.edu.vn

2nd Duong Duc Ha
Le Quy Don Technical University
 Ha Noi, Viet Nam
 duongha@mta.edu.vn

3rd Pham Thanh Hiep
Le Quy Don Technical University
 Ha Noi, Viet Nam
 phamthanhiep@gmail.com

Abstract—With the very larger bandwidth, the ultra-wide band (UWB) technology has good resolution when used for short-range positioning techniques and the correct detection of the received UWB signals is one of the important factors affect the accuracy of the positioning technique. In this paper, a method used to improve the detection accuracy of the received UWB signal in multi-path environment based on the synthesize sample waveform at the UWB receiver is proposed. The results obtained from the mathematic analysis and computer simulation show that with the proposed technique, the ability to detect the UWB signal is improved, the effect of inter pulse interference (IPI) is eliminated, and the accuracy in measuring the distance is enhanced.

Index Terms—Gaussian monocycle, IR-UWB, template waveform.

I. INTRODUCTION

UWB technology currently used in wireless communication networks such as wireless personal area networking (WPAN), indoor, outdoor positioning network, automotive tracking systems, etc. UWB systems can provide high data rates, large capacities, and high accuracy with short-range positioning techniques due to their very larger bandwidth. According to the definition of United States Federal Communications Commission (FCC) in which a UWB signal occupies in a bandwidth of 500 MHz or more, so it has a resolution of centimeter [1].

The UWB positioning technology based on the parameters related to the distance of the received signal such as angle of arrival (AOA) [2], received signal strength (RSS) [3], time of arrival (TOA) [4], and time difference of arrival (TDOA) [5]. In those, the TOA/TDOA-based methods take advantage of the high resolution of the UWB signal, thus satisfying the requirement of precise positioning [6]. Hence, the TOA-based distance determination method is used in this paper.

There are two dominant technologies for UWB system. One is a multi-band technique that uses modulated signals to achieve the desired bandwidth; and the other is the impulse radio UWB signal (IR-UWB) technique [7] [8]. Many pulse shapes have been applied for IR-UWB technology, such as monocycle Gaussian pulse [7], Modified Hermite Pulse (MHP) with the Pulse Shape Modulation (PSM) scheme [9] [10]. In addition, other orthogonal polynomials have also been studied to generate pulse shapes used in UWB technology [11] [12]. The IR-UWB system uses extremely short sub-second pulses

and has a large number of resolvable multi-path components in the received signal [13].

In order to detect the reflected UWB pulses, conventional receivers typically use a matched filtering technique where it is necessary to generate a sample waveform with the same pulse shape as the received pulse. Therefore, the matched filtering techniques at the receiver can only detect the specified UWB pulse and not any other type of UWB signal. Furthermore, in the PSM scheme using orthogonal pulses such as the Modified Hermite pulse, there is a disadvantage that separate waveform generators are required when transmitting and receiving [10]. The template waveform of the correlator in UWB system can be specially designed based on the window method to suppress interference without knowledge of the phases or amplitudes of the interference presented in [14]. This method is applied to UWB systems without the influence of multi-path.

The multi-path effect affects the direct path detection of the received UWB signal, thereby causing TOA estimation error. Identifying and eliminating the IPI introduced by multi-path is one of the difficulties to improve the accuracy of UWB positioning system. The multi-carrier-based sample waveforms have been investigated to reduce interference in studies [15] [16] [17]. The timing with dirty templates for UWB system is proposed in [18] can achieve high synchronization and low system complexity requirements. However, this method is only applicable provided that there is no inter symbol interference (ISI). Digital techniques such as equalizers and Rake receiver [19] can be used to eliminate the influence of IPI. However, due to the very larger bandwidth of IR-UWB signal, it is very difficult to digitize IR-UWB signals, resulting in increased complexity and power consumption of UWB system [20]. All of these have caused obstacles to IPI removal, leading to large errors in the UWB positioning system.

To eliminate the influence of IPI and increase the accuracy of distance measurement of UWB positioning systems in multi-path environments, this paper proposes a method of synthesizing the adaptive template waveforms at the correlator of receiver. The template waveform was generated by combining the orthogonal fundamental Gaussian functions with the coefficients that can be adjusted. By determining the value of the coefficient of each component Gaussian function, the suitable template waveform can be synthesized and used to increase accuracy in TOA estimation and propagation distance

determination.

The next part of the paper is organized as follows: Sect. II describes the system model, the proposed sample waveform synthesis technique is presented in Sect. III, Sect. IV shows the numerical results and the paper is concluded in Sect. V.

II. SYSTEM MODEL

A typical penetrating IR-UWB system is illustrated in Fig. 1. The transmission medium has the relative permittivities are ϵ . The transmitted signal is IR-UWB denoted as $s(t)$ and the reflected from the buried object denoted as $r(t)$. A IR-UWB

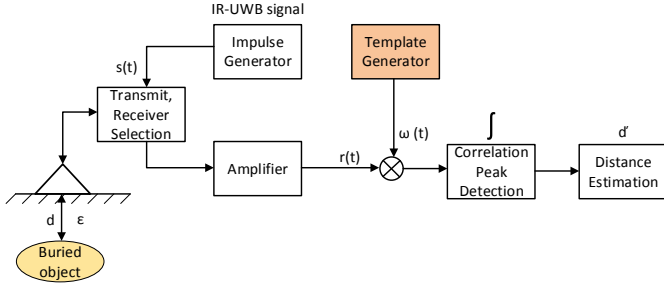


Fig. 1. The penetrating IR-UWB system.

signal takes the form [21]:

$$s_{IR}(t) = \sqrt{P} \sum_{i=0}^{N_p} g(t - iT_r), \quad (1)$$

where t is time, P is the transmit power, N_p is the number of transmitted pulses, $g(t)$ is the signal pulse with pulse width T ; T_r is the repetitive period of the pulse. In this paper, the signal pulses used are derivatives of the basic Gaussian pulse named Gaussian monocycles with n^{th} order is:

$$g_n(t) = B_{np} \frac{d^n}{dt^n} e^{-2\pi(\frac{t}{\mu_p})^2}, \quad (2)$$

where μ_p is a time normalization factor and B_{np} is normalized energy of $g_n(t)$. In the multi-path transmission, the received signal has the forms:

$$r(t) = A \sum_{m=0}^M A_m s(t - m\tau_p) + n(t), \quad (3)$$

where A is the amplitude of multi-path channel with a log-normal distribution, A_m represents the amplitude of the m^{th} path, τ_p is the minimum resolution, M is the total number of paths that can be processed for each reflected signal, and $n(t)$ is the Gaussian noise. At the receiver side, the reflected signal $r(t)$ is correlated with the template waveforms to determine the delay time by the correlation peaks. With the assumption that the synchronization between the transmitter and the receiver can be achieved perfectly, the correlation output according to the m^{th} path of the i^{th} pulse is represented as:

$$R_i^m = \int_{-\frac{T}{2} + (iT_r + m\tau_p)}^{\frac{T}{2} + (iT_r + m\tau_p)} r(t) \omega(t - iT_r - m\tau_p) dt + n_i^m, \quad (4)$$

where T , $\omega(t)$, $(iT_r + m\tau_p)$, n_i^m are the pulse width, the desired sample waveform, the time delay of the reflected signal, and the Gaussian noise, respectively.

In case the pulse width exceeds the minimum resolution of the multi-path ($T > \tau_p$), the overlapping will occur in the reflected pulses at the receiver, called interference inter impulses (IPI). Under the influence of IPI, the reflected pulses will be distorted, so the sample waveforms at the receiver are no longer suitable for the correlation determination. The distorted signal waveform due to IPI is shown in Fig. 2 The

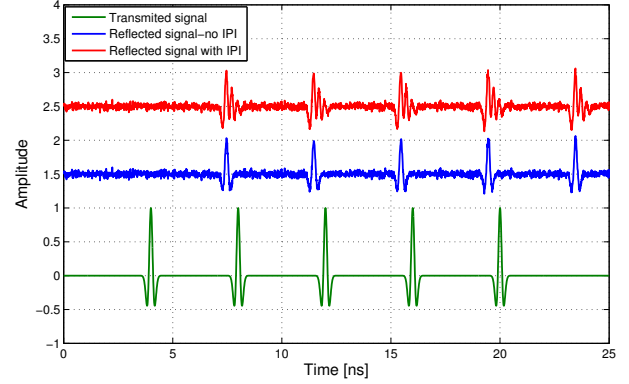


Fig. 2. The transmitted and reflected signal waveforms.

number of multipath components inside the pulse width can be calculated:

$$K = \text{floor}\left(\frac{T}{\tau_p}\right) \quad (5)$$

The floor function in Eq. (5) used to get the integer part of (T/τ_p) . The desired correlation output corresponding to the m^{th} path of the i^{th} pulse is:

$$R_{di}^m = \sqrt{PA} \sum_{l=0}^K \left\{ A_{m+l} \int_{-\frac{T}{2}}^{\frac{T}{2}} g(t) \omega(t - l\tau_p) dt \right\}. \quad (6)$$

Eq.(6) can be represented as follows.

$$R_{di}^m = \sqrt{PA} \sum_{l=0}^K \left\{ A_{m+l} R_{g\omega}(l\tau_p) \right\}, \quad (7)$$

where

$$R_{g\omega}(\tau) = \int_{-\frac{T}{2}}^{\frac{T}{2}} g(t) \omega(t - \tau) dt. \quad (8)$$

In Eq. (6), the components $l = 1, \dots, K$ represent the effect of IPI. Under the influence of IPI, the transmitted waveform $g(t)$ will no longer be suitable to be used as the sample waveform $\omega(t)$ at the receiver side. In order to reduce the influence of IPI in the correlation calculation on the negative side, the template waveforms synthesize technique based on combining orthogonal fundamental waveforms with certain coefficients is proposed.

III. THE SAMPLE WAVEFORM SYNTHESIS TECHNIQUE

A. Proposal the model of template waveform generation

The proposed model for generating the template waveforms is illustrated in Fig. 3. The UWB sample waveform is gener-

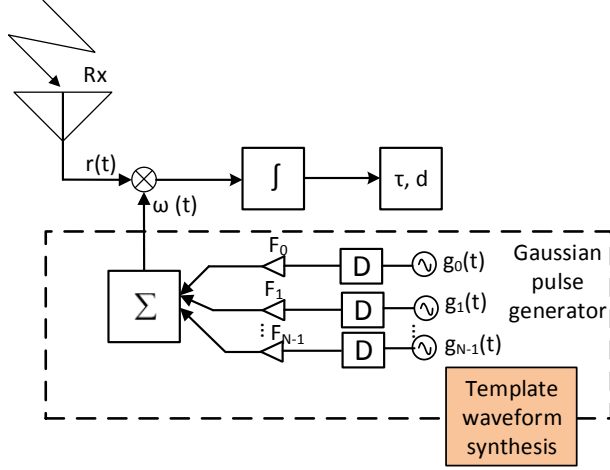


Fig. 3. The proposed model for generating the template waveforms

ated by combining several elementary waveforms:

$$\omega(t) = \sum_{i=0}^{K-1} F_i g_i(t - i\tau_p), \quad (9)$$

where $g_i(t)$ are Gaussian monocycles, the coefficients F_i are calculated such that the mean deviation value Eq. (10) gets the smallest value.

$$MD(\mathbf{F}) = \frac{1}{T} \int_{-\frac{T}{2}}^{\frac{T}{2}} \left[r(t) - \sum_{i=0}^{K-1} F_i g_i(t - i\tau_p) \right]^2 dt. \quad (10)$$

B. Determining coefficients algorithm

To determine the values of F_i , the Eq. (10) is rewritten as

$$MD(\mathbf{F}) \approx \frac{1}{Q} \sum_{k=1}^Q \left[r(t_k) - \sum_{i=0}^{K-1} F_i g_i(t_k - i\tau_p) \right]^2, \quad (11)$$

where Q is the number of discrete points in the Eq. (11) and

$$t_k = k \cdot \frac{T}{Q}. \quad (12)$$

The coefficients F_i are determined to satisfy the minimum mean squared error (MMSE) criterion in Eq. (11) by using Gauss-Newton method [22] and illustrated in the diagram shown in Fig. 4. In Fig. 4, the vector $\mathbf{F} = \{F_0, F_2, \dots, F_{K-1}\}$ is initialized with a random value in the interval (0,1) and calculated after 50 iterations by Gauss-Newton algorithm for each value of K . After that, the value of the mean deviation MD is calculated according to the Eq. (11). For each K , the local minimum value MD_K is determined and compared with a threshold value δ_{th} , the final result of \mathbf{F} vector corresponding to the minimum value of MD_K . The updated step vector $\Delta\mathbf{F}$

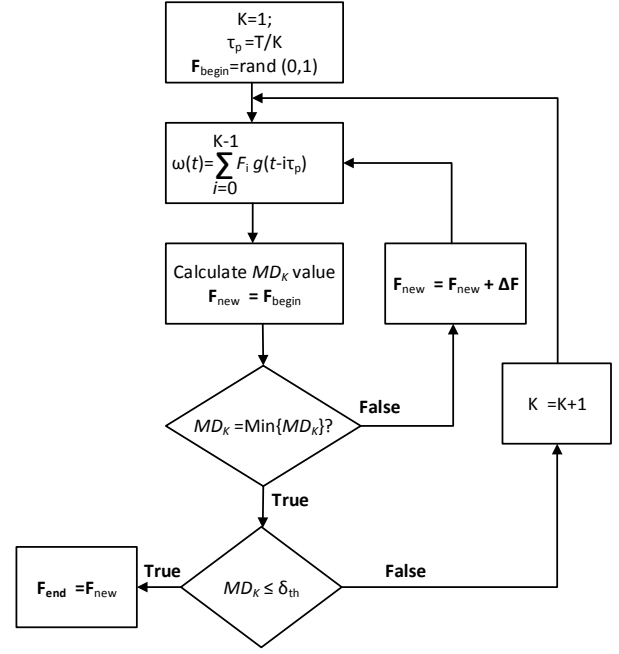


Fig. 4. The diagram of the propose algorithm

for the $(s+1)^{th}$ iteration ($s+1$ runs from 1 to 50) is determined by Gauss-Newton algorithm as follows.

$$\Delta\mathbf{F} = \mathbf{F}^{(s+1)} - \mathbf{F}^{(s)} = -(\mathbf{J}^H \mathbf{J})^{-1} \mathbf{J}^H \mathbf{MD}(\mathbf{F}^{(s)}), \quad (13)$$

where, \mathbf{J} is the Jacobian matrix, if \mathbf{MD} and \mathbf{F} are column vectors, the entries of \mathbf{J} are:

$$\mathbf{J}_{kl} = \frac{\partial MD_k(\mathbf{F}^{(s)})}{\partial F_l}, \quad (14)$$

where

$$MD_k(\mathbf{F}^{(s)}) = r(t_k) - \sum_{i=0}^{K-1} F_i^{(s)} g_i(t_k - i\tau_p). \quad (15)$$

Ignoring the influence of Gaussian noise, the sample waveforms after synthesis are evaluated by the normalized mean square error (NMSE) criterion:

$$MSEN = \sqrt{\frac{\int_{-\frac{T}{2}}^{\frac{T}{2}} \left[r(t) - \sum_{i=0}^{K-1} F_i g_i(t - i\tau_p) \right]^2 dt}{\int_{-\frac{T}{2}}^{\frac{T}{2}} r(t)^2 dt}}. \quad (16)$$

IV. NUMERICAL RESULTS AND COMPARISONS

All the numerical results in this paper were computed using Matlab. The parameters of an example UWB system are listed in the Tab. I with using the second Gaussian monocycle.

TABLE I
SIMULATION PARAMETERS [23]

| Parameter | Notation | Value |
|---------------------------|---------------|----------------|
| Impulse Width | T | 0.7 ns |
| Time normalization factor | μ_p | 0.2877 ns |
| Effective bandwidth | ΔF | 3.5 GHz |
| Pulse repetition cycle | T_r | 50 ns |
| Number of multi-path | K | 2, 3, 4 |
| Number of pulses | N_p | 100 |
| Number of discrete point | Q | 100 |
| The threshold value | δ_{th} | 0.01 |
| The relative permittivity | ϵ | 4.5 (dry sand) |

A. The result of the sample waveform synthesis algorithm

The effect of the number of component pulses on the sample waveform illustrated in Fig. 5. Using the coefficients method, the synthesized template waveform can be constructed with several Gaussian monocycle. The performance of proposed method depends on the choice of the number of Gaussian monocycles and the threshold value. The smaller threshold value lead the better approximation, however, the computation time and complexity of algorithm will be increased significantly. In Fig. 5, it can be seen that even under the IPI environment, the proposed synthesized template waveform is more closely represents the received signal, and hence the accuracy of distance estimation in positioning will be improved. Fig. 6

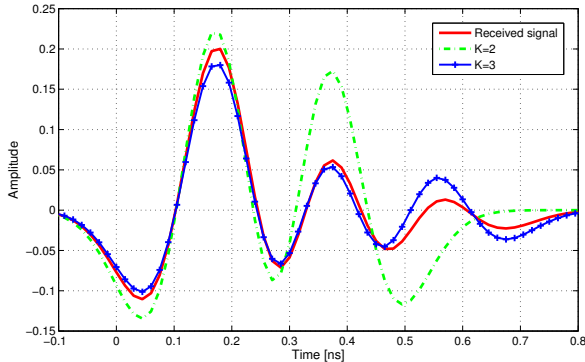


Fig. 5. The received signal and the synthesized template waveforms

shows the NMSE value which is calculated by Eq. (16) and it depends on the number of the Gaussian monocycles used to synthesize the sample waveform, the NMSE decreases as the number of Gaussian monocycles increases.

B. Measuring the distance

The propagation distance is estimated based on the maximum value of the correlation function in Eq. (4). Assuming that the wave propagation medium is homogeneous and has a dielectric constant of ϵ . The propagation distance is calculated from the delay time τ , the speed of light c and ϵ by the Eq. (17) [24].

$$d = \frac{c\tau}{\sqrt{\epsilon}}. \quad (17)$$

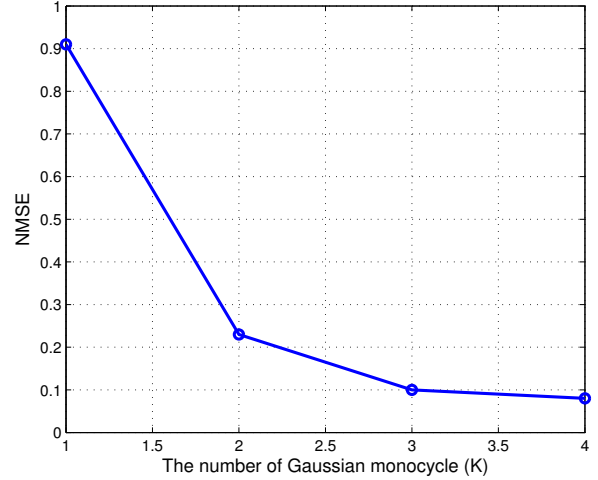


Fig. 6. The NMSE of the synthesized waveform

where, the delay time τ is determined such that the correlation output in Eq. (8) reach the maximum value:

$$\tau = \text{Arg max}_{\tau} R_{g\omega}(\tau). \quad (18)$$

The synthesized sample waveform used to estimate the propagation distance in the positioning model is illustrated in Fig. 1 for the case of a multipath transmission medium with IPI.

The error of distance estimation is illustrated in Fig. 7, where the estimation error is determined by the equation:

$$\text{err} = |d_{est} - d_{real}|, \quad (19)$$

where d_{est} is the average estimated distance, d_{real} is the actual value. In Fig. 7, when the synthesized waveform is more

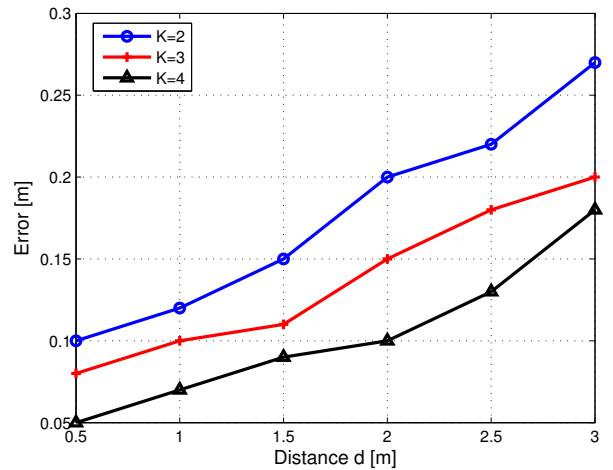


Fig. 7. Distance estimation error when changing sample waveforms

similar to the received signal (K increases), the estimation error decreases, specifically with the number of the Gaussian monocycle $K = 2$, with $d_{real} = 2[m]$, the estimation error

is 0.2[m]; with $K = 4$, the error is reduced to 0.1[m]. The root mean squared error (RMSE) of the proposed method in determining the delay time τ can be calculated by:

$$RMSE = \sqrt{\frac{1}{N} \sum_{k=1}^N (\hat{\tau}_k - \tau)^2}, \quad (20)$$

where N is the number of iterations of the delay time calculations, $\hat{\tau}_k$ is the estimated value at the k^{th} computation.

To evaluate the results of the delay time estimation, the estimated values are compared with the Cramer-Rao lower bound (CRLB) on the standard deviation of an unbiased TOA estimator $\hat{\tau}$. The CRLB is given by [25]:

$$\sqrt{Var(\hat{\tau})} \geq \frac{1}{2\sqrt{2}\pi\sqrt{SNR}\Delta F}, \quad (21)$$

where SNR, ΔF are signal to noise ratio and effective bandwidth, respectively. The change of RMSE vs. SNR with different template waveforms used in estimating the delay time τ is illustrated in Fig. 8 with the distance $d = 2$ m.

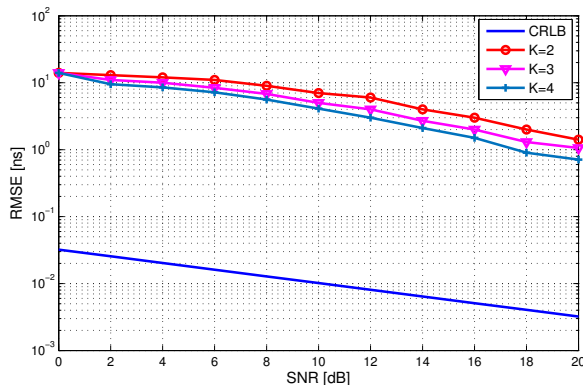


Fig. 8. RMSE of estimated delay time in comparison with CRLB

V. CONCLUSION

This paper proposes a method of synthesizing adaptive template waveforms at the correlator of the positioning UWB system under the influence of IPI. The template waveform was synthesized based on the fundamental Gaussian functions. The coefficient of each Gaussian function was estimated using the Gauss-Newton algorithm. The proposed method is evaluated in terms of the error of estimated distance when using the synthesized template waveforms for the UWB positioning system. The simulation results show that the proposed method can be used to increase the accuracy of distance measurement and avoid the influence of IPI in the UWB positioning system in the multi-path environment.

REFERENCES

- [1] Cook, Charles. Radar signals, "An introduction to theory and application," Elsevier, 2012.
- [2] Diagne, Salick, "Performances analysis of a system of localization by angle of arrival UWB radio," International journal of communications, network and system sciences, vol. 13, No.2, pp. 15-27, 2020.

- [3] D. Zhu and K. Yi, "EKF localization based on TDOA/RSS in underground mines using UWB ranging," in Proc. IEEE Int. Conf. Signal Process., Commun. Comput., Sep. 2011, pp. 1–4.
- [4] I. Guvenc, Z. Sahinoglu, and P. Orlik, "TOA estimation for IR-UWB systems with different transceiver types, IEEE Trans. Microw. Theory Techn., vol. 54, no. 4, pp. 1876–1886, Jun. 2006.
- [5] R. Fujiwara, K. Mizugaki, T. Nakagawa, D. Maeda, and M. Miyazaki, "TOA/TDOA hybrid relative positioning system based on UWB-IR technology, IEICE Trans. Commun., vol. E94.B, no. 4, pp. 1016–1024, 2011.
- [6] Z. Yin, K. Cui, Z. Wu, and L. Yin, "Entropy-based TOA estimation and SVM-based ranging error mitigation in UWB ranging systems, Sensors, vol. 15, pp. 11701–11724, May 2015.
- [7] Vojcic, Branimir R., and Raymond L. Pickholtz, "Direct-sequence code division multiple access for ultra-wide bandwidth impulse radio," IEEE Military Communications Conference, 2003. MILCOM 2003. Vol. 2. IEEE, 2003.
- [8] Win, Moe Z., and Robert A. Scholtz, "Impulse radio: How it works." IEEE Communications letters 2.2, pp. 36–38, 1998.
- [9] Michael, Lachlan B., Mohammad Ghavami, and Ryuji Kohno, "Multiple pulse generator for ultra-wideband communication using Hermite polynomial based orthogonal pulses," 2002 IEEE Conference on Ultra Wideband Systems and Technologies (IEEE Cat. No. 02EX580). IEEE, 2002.
- [10] De Abreu, Giuseppe Thadeu Freitas, Craig John Mitchell, and Ryuji Kohno, "On the orthogonality of hermite pulses for ultra wideband communications systems," rn 1000, 2003.
- [11] Pinchas, M., "Orthogonal laguerre polynomial pulses for ultra-wideband communications," Proc. IWUWBS'03, Oulu, Finland, June (2003).
- [12] Ciolino, S., "UWB pulse shape modulation system using wavelet packets," Proc. International Workshop on Ultra Wideband Systems (IWUWBS'03), Oulu, Finland, June, 2003.
- [13] L. Chao, W. Xuanli, and C. Yang, "Multipath interference analysis of IR-UWB systems in indoor office LOS environment, in Proc. 6th Int. ICST Conf. Commun. Netw. China, 2011, pp. 846–850.
- [14] Wang, X., Lin, F., Jia, W. K., "Interference Cancellation for Software Defined Impulse Radio by Template Design. In NOMS IEEE/IFIP Network Operations and Management Symposium, pp. 1-5. IEEE, April, 2020.
- [15] Ohno, Kohei, "Effect of interference from other radio system to UWB impulse radio," Proc. IWUWBS'03, Oulu, Finland, June (2003).
- [16] Ohno, Kohei, Takanori Ikebe, and Tetsushi Ikegami, "A proposal for an interference mitigation technique facilitating the coexistence of biphas UWB and other wideband systems," 2004 International Workshop on Ultra Wideband Systems Joint with Conference on Ultra Wideband Systems and Technologies. Joint UWBST, IWUWBS 2004 (IEEE Cat. No. 04EX812). IEEE, 2004.
- [17] Moon, Todd K., and Wynn C. Stirling, "Mathematical methods and algorithms for signal processing," No. 621.39: 51 MON. 2000.
- [18] Yang, Liuqing, and Georgios B. Giannakis, "Timing ultra-wideband signals with dirty templates," IEEE Transactions on communications, vol. 53, No.11, pp. 1952–1963, 2005.
- [19] A. Klein, D. Brown, D. Goeckel, and C. Johnson, "RAKE reception for UWB communication systems with intersymbol interference, in Proc. 4th IEEE Workshop Signal Process. Adv. Wireless Commun., Rome, Italy, 2003, pp. 244–248.
- [20] G. Yue, Z. Wang, and H. Yin, "Performance of monobit digital receivers with inter-symbol interference, IEEE Wireless Commun. Lett., vol. 3, no. 1, pp. 66–69, Feb. 2014.
- [21] Sahinoglu, Zafer and Gezici, Sinan and Guvenc, Ismail, "Ultra-wideband positioning systems, Cambridge, New York, 2008.
- [22] Björck, Åke, "Numerical methods for least squares problems, Society for Industrial and Applied Mathematics, 1996.
- [23] B. Hu and N. C. Beaulieu, "Accurate evaluation of multiple-access performance in th-ppm and th-bpsk uwb systems, IEEE Transactions on communications, vol. 52, No. 10, pp. 1758–1766, 2004.
- [24] Gottlieb, Irving M, "Practical RF power design techniques, Tab Books, 1993.
- [25] Soganci, Hamza and Gezici, Sinan and Poor, H Vincent, "Accurate positioning in ultra-wideband systems, IEEE Wireless Communications, vol. 18, no. 2, pp. 19–27, 2011.